I&EC research
Industrial & Engineering Chemistry Research

Article

pubs.acs.org/IECR

Fault-Tolerant Economic Model Predictive Control Using Error-Triggered Online Model Identification

Anas Alanqar,[†] Helen Durand,[†] and Panagiotis D. Christofides*[,†,‡]

[†]Department of Chemical and Biomolecular Engineering, University of California, Los Angeles, California 90095, United States
[‡]Department of Electrical Engineering, University of California, Los Angeles, California 90095, United States

ABSTRACT: In this work, we present a data-driven methodology to overcome actuator faults in empirical model-based feedback control. More specifically, we introduce the use of a moving horizon error detector that quantifies prediction errors and triggers updating of the model used in the controller online when significant prediction errors occur due to the loss of one of the actuators. Model reidentification is conducted online using the most recent input/output data collected after the fault occurrence. The error-triggered online model identification approach can be applied to overcome various types of actuator faults, including the case where the value at which the actuator is stuck is known and the case where the value at which the actuator is stuck is unknown. The proposed methodology is applied in an economics-based feedback controller, termed economic model predictive control (EMPC), that uses a model obtained either from first-principles or from plant data to optimize plant economics online. Two different chemical process examples are considered in order to demonstrate the application of the proposed strategy. In the first example, application of the proposed scheme for the case where the value at which the actuator is stuck is known is demonstrated through a benchmark catalytic chemical reactor example where the actuator faults occur in the heat input causing shifts and variations in plant operating conditions. The second example demonstrates the case where the value at which the actuator is stuck is unknown. The proposed scheme was able to compensate for the variations in the plant caused by the actuator loss by obtaining more accurate models that are suitable for the new conditions and updating them in the EMPC architecture. Improved economic performance was obtained as the updated models were able to capture the process dynamics under the new conditions and provide better state predictions.

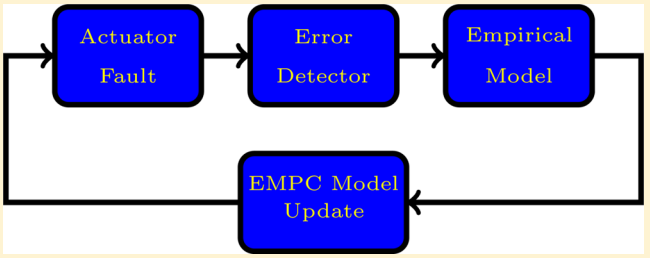

INTRODUCTION

Recent technological developments in the chemical and petrochemical industries have led to the creation of complex process networks to increase operational efficiency and meet the increasing energy demand. One approach for maximizing the efficiency of process operation is by integrating process control and process economic optimization. Economic model predictive control (EMPC) is a recent model-based feedback control strategy that integrates process control with dynamic economic optimization of the plant. EMPC promotes optimal time-varying operation of the plant and can incorporate constraints that ensure closed-loop stability (e.g., refs 1−4).

The first step in developing model-based feedback controllers is to establish a dynamic model representing the process dynamics, which can be done either from first-principles or through system identification.[5] While first-principles models describe the underlying physicochemical phenomena and develop detailed mathematical expressions for the observed process mechanisms, obtaining such models is a challenging task for complex and poorly understood processes. Instead, model identification provides suitable alternative models to be used for model-based feedback control when first-principles models are too complex or unavailable. Over the past four decades, various model identification methods have been developed to identify linear and nonlinear models from process data alone (e.g., refs 5−7).

Subspace model identification (SMI) refers to a class of system identification methods that are capable of identifying multiple-input multiple-output (MIMO) models based purely on input/output data.[7−11] SMI methods are noniterative and account for multivariable interactions.[7,12] Well-recognized SMI methods include numerical algorithms for subspace state-space system identification (N4SID),[12] the Canonical Variate Algorithm (CVA),[13] and the multivariable output error state-space (MOESP) algorithm.[8,10] SMI methods have been widely used for industrial applications due to their reliability and numerical stability.[6,8,9,14] SMI methods have been used to provide models for various model-based feedback control systems such as model predictive control (MPC) and EMPC.[11,15]

A major problem that arises frequently in the chemical industry is actuator faults, in which authority over one or more actuators is lost. Detecting actuator faults and developing advanced fault-tolerant controllers for chemical process systems

Received: February 9, 2017
Revised: April 24, 2017
Accepted: April 26, 2017
Published: April 26, 2017

DOI: 10.1021/acs.iecr.7b00576
Ind. Eng. Chem. Res. 2017, 56, 5652−5667

has been previously considered (e.g., in refs 16 and 17). However, the existing works have assumed the availability of a first-principles model to develop fault-tolerant control methodologies. To date, to the best of our knowledge, no work on formulating fault-tolerant control strategies using empirical models has been considered. In the present work, we introduce a data-driven approach to overcome actuator faults in Lyapunov-based economic model predictive control (LEMPC) based on linear empirical models, which can be extended to other model-based feedback control designs. When actuator faults cause the prediction errors between the predicted states from the linear empirical model and the measured states to increase, model reidentification is triggered online by a moving horizon error detector if an error metric exceeds a prespecified threshold. The proposed methodology is applied to two different chemical process examples to demonstrate the ability of the detector to indicate significant prediction errors when actuator faults occur and update the model online in order to obtain more accurate predictions. The first example considers the application of the proposed scheme for the case where the value at which the actuator is stuck is known in a benchmark catalytic chemical reactor example where the actuator faults occur in the heat input causing shifts and variations in plant operating conditions. The second example demonstrates the application of the proposed scheme for the case where the value at which the actuator is stuck is unknown. Improved state predictions and economic performance were obtained by the proposed scheme as the updated models were able to capture the process dynamics and compensate for the variations in the plant caused by the actuator loss.

PRELIMINARIES

Notation. The operator $|\cdot|$ is used to denote the Euclidean norm of a vector. The transpose of a vector x is denoted by the symbol x^T. The symbol Ω_ρ represents a level set of a positive definite continuously differentiable scalar-valued function $V(x)$ ($\Omega_\rho := \{x \in R^n: V(x) \le \rho\}$). A continuous function $\alpha: [0,a) \to [0,\infty)$ is said to belong to class $\mathcal{K}$ if it is strictly increasing and is zero only when evaluated at zero. The symbol diag(a) denotes a square diagonal matrix where the diagonal elements are the components of the vector a. The sampling period is denoted as $\Delta > 0$.

Class of Systems. This work considers a broad class of process systems described by first-order nonlinear ordinary differential equations of the following form:

$$\dot{x}(t) = f(x(t), u(t), w(t)) \tag{1}$$

where $x \in R^n$, $u \in R^m$, and $w \in R^l$ are the state vector of the system, the manipulated input vector, and the disturbance vector, respectively. The disturbance vector is assumed to be bounded (i.e., $|w(t)| \le \theta$ for all t). Physical limitations on actuation energy restrict the manipulated inputs to belong to the convex set $U := \{u \in R^m: u_i^{\min} \le u_i \le u_i^{\max}, i = 1, ..., m\}$. The function f is assumed to be locally Lipschitz, and the origin is taken to be an equilibrium of the nominal unforced system of eq 1 (i.e., $f(0,0,0) = 0$). We assume that state measurements $x(t_k)$ are available at each sampling time $t_k = k\Delta$, $k = 0, 1, ...$

This work is restricted to the class of stabilizable nonlinear systems. Specifically, we assume the existence of a locally Lipschitz feedback control law $h(x) \in U$ that can render the origin of the nominal ($w(t) \equiv 0$) closed-loop system of eq 1 locally asymptotically stable in the sense that there exists a continuously differentiable Lyapunov function $V: R^n \to R_+$ where the following inequalities hold:[18,19]

$$\alpha_1(|x|) \le V(x) \le \alpha_2(|x|) \tag{2a}$$

$$\frac{\partial V(x)}{\partial x} f(x, h(x), 0) \le -\alpha_3(|x|) \tag{2b}$$

$$\left|\frac{\partial V(x)}{\partial x}\right| \le \alpha_4(|x|) \tag{2c}$$

for all x in an open neighborhood D that includes the origin in its interior and $\alpha_j(\cdot)$, $j = 1, 2, 3, 4$, are class $\mathcal{K}$ functions. For various classes of nonlinear systems, several stabilizing control laws have been developed that take input constraints into consideration.[20−22] The stability region of the closed-loop system is defined to be a level set $\Omega_\rho \subset D$ where $\dot{V} < 0$. The origin of the closed-loop system is rendered practically stable when the control law $h(x)$ is applied in a sample-and-hold fashion for a sufficiently small sampling period.[23]

In this work, we apply an online model identification scheme to obtain empirical models that capture the evolution of the system of eq 1. The empirical models obtained are linear time-invariant (LTI) state-space models of the form

$$\dot{x}(t) = A_i x(t) + B_i u(t) \tag{3}$$

where the constant matrices $A_i \in R^{n\times n}$ and $B_i \in R^{n\times m}$ correspond to the ith model identification performed ($i = 1, ..., \tilde{M}$). We assume the existence of a set of stabilizing control laws $h_{L1}(x)$, $h_{L2}(x)$, ..., $h_{L\tilde{M}}(x)$ designed based on the empirical models that can make the origin of the closed-loop system of eq 1 asymptotically stable and generate a continuously differentiable Lyapunov function $\hat{V}: R^n \to R_+$ where the following inequalities hold:[19]

$$\hat{\alpha}_1(|x|) \le \hat{V}(x) \le \hat{\alpha}_2(|x|) \tag{4a}$$

$$\frac{\partial \hat{V}(x)}{\partial x} f(x, h_{Li}(x), 0) \le -\hat{\alpha}_{3_i}(|x|), \quad i = 1, \ ..., \ \tilde{M} \tag{4b}$$

$$\left|\frac{\partial \hat{V}(x)}{\partial x}\right| \le \hat{\alpha}_4(|x|) \tag{4c}$$

for all x in an open neighborhood D_{Li} that includes the origin in its interior. The functions $\hat{\alpha}_j(\cdot)$, $j = 1, 2, 4$, and $\hat{\alpha}_{3_i}$, $i = 1, ..., \tilde{M}$, are class $\mathcal{K}$ functions, and the stability region of the system of eq 1 under the controller $h_{Li}(x)$ is defined as the level set $\Omega_{\hat{\rho}_i} \subset D_{Li}$, $i = 1, ..., \tilde{M}$.

Lyapunov-Based EMPC. The formulation of EMPC to be used in this work incorporates Lyapunov-based stability constraints based on the explicit stabilizing controller $h(x)$. The resulting Lyapunov-based EMPC (LEMPC)[3] maximizes an economics-based cost function representing the plant economics and is given by the following optimization problem:

$$\min_{u\in S(\Delta)} \int_{t_k}^{t_{k+N}} L_e(\tilde{x}(\tau), u(\tau))\, d\tau \tag{5a}$$

$$\text{s.t. } \dot{\tilde{x}}(t) = f(\tilde{x}(t), u(t), 0) \tag{5b}$$

$$\tilde{x}(t_k) = x(t_k) \tag{5c}$$

$$u(t) \in U, \forall\ t \in [t_k, t_{k+N}) \tag{5d}$$

DOI: 10.1021/acs.iecr.7b00576
Ind. Eng. Chem. Res. 2017, 56, 5652−5667

$$V(\tilde{x}(t)) \le \rho_e, \quad \forall\ t \in [t_k, t_{k+N}) \quad \text{if} \quad x(t_k) \in \Omega_{\rho_e} \tag{5e}$$

$$\frac{\partial V(x(t_k))}{\partial x} f(x(t_k), u(t_k), 0) \le \frac{\partial V(x(t_k))}{\partial x} f(x(t_k), h(x(t_k)), 0) \quad \text{if} \quad x(t_k) \notin \Omega_{\rho_e} \tag{5f}$$

where the decision variables are the input trajectories over the prediction horizon $N\Delta$ (i.e., $u \in S(\Delta)$ where $S(\Delta)$ signifies the class of piecewise-constant functions with period Δ). Control actions are implemented in a receding horizon fashion using process state predictions $\tilde{x}(t)$ from the dynamic model of the process (eq 5b) initiated from the state feedback measurement at each sampling time (eq 5c). Input constraints are taken into consideration in the LEMPC formulation in eq 5d.

The Mode 1 constraint (eq 5e) is activated when the state measurement is maintained within a subset of the stability region Ω_ρ that is referred to as Ω_{ρ_e}, and promotes time-varying process operation to maximize economics. When the closed-loop state exits Ω_{ρ_e}, the Mode 2 constraint (eq 5f) is activated to force the state back into Ω_{ρ_e} by computing control actions that decrease the Lyapunov function value. The stability region subset Ω_{ρ_e} is chosen to make Ω_ρ forward invariant in the presence of process disturbances.

EMPC USING ERROR-TRIGGERED ONLINE MODEL IDENTIFICATION

The potential of EMPC for improving profits in the chemical process industries has motivated research in practical aspects of EMPC implementation, including the use of linear empirical models in EMPC.[15,24] However, all work on improving the practicality of EMPC with empirical models has assumed that no actuator faults occur, though the development of actuator faults poses unique challenges for linear empirical models utilized to obtain state predictions within EMPC. Because the models are developed with all actuators online based on process data only, there is no guarantee that, when the underlying process dynamics change (i.e., an actuator output becomes fixed when it was previously varying), the model developed based on data for the case that all actuators were varying will remain valid with the value of the faulty actuator fixed for all time, since this condition was not included in the original process data used to identify the model and the underlying process model is typically nonlinear such that nonlinear and coupled interactions between states and inputs exist. This can impact the accuracy of state predictions utilized within the EMPC after the fault occurs, which can negatively impact process profits as well as satisfaction of other constraints (including stability or state constraints). Though reidentification of the model when the fault is detected may appear to be a solution to the potential problems caused by the fault for the accuracy of the linear empirical models, reidentification would require the availability of a sufficient number of input/output data points corresponding to the new (after fault) operating conditions. Since sufficient after-fault data for model reidentification is not available until after the fault, there will be some time period during which the empirical model developed from data corresponding to the case that all actuators are online must continue to be utilized within the EMPC. Furthermore, depending on the severity of the fault and the empirical model in use at the time of the fault, the original empirical model may provide sufficiently accurate state predictions such that it is not necessary to interrupt the continuity of the control strategy by updating the model used within the controller. Therefore, a method for determining when the model should be updated as a result of the fault is necessary. In this work, we propose the use of the moving horizon error detector developed in ref 24 for this task; however, important changes to the implementation strategy of the LEMPC with error-triggered online model identification from ref 24 must be made to address the issues specific to faults discussed above. In this development, we assume that a fault has occurred in an actuator that causes the actuator output to take some value, where it is known which actuator has experienced a fault. The proposed approach to develop fault-tolerant control for empirical model-based LEMPC may be applied in the case where the value of the faulty actuator's output is known and in the case where the value of the faulty actuator's output is unknown. We make no requirement on the number of faults that can occur at one time, as long as the number of online actuators allows sufficiently accurate linear empirical models to continue to be identified (observability assumption). Therefore, this method is flexible to handle multiple actuators experiencing faults simultaneously (and can also be extended to include recommissioning of actuators that experienced faults and have been repaired) throughout time. The following section presents the LEMPC formulation using linear empirical models. After that, the formulation of the moving horizon error detector and the implementation strategy for online model identification to compensate for changes in the model due to actuator faults are introduced.

LEMPC Formulation Using Empirical Models. In this work, it is assumed that the plant model of eq 1 is unavailable and the process model to be incorporated in the LEMPC design is the ith empirical model ($i = 1, ..., \tilde{M}$). The empirical models and their corresponding $h_{Li}(x)$ and $\hat{V}(x)$ are used in the development of the stability constraints. The LEMPC design using the ith empirical model is presented by the following optimization problem:[15]

$$\min_{u \in S(\Delta)} \int_{t_k}^{t_{k+N}} L_e(\hat{x}(\tau), u(\tau))\, d\tau \tag{6a}$$

$$\text{s.t. } \dot{\hat{x}}(t) = A_i \hat{x}(t) + B_i u(t) \tag{6b}$$

$$\hat{x}(t_k) = x(t_k) \tag{6c}$$

$$u(t) \in U, \quad \forall\ t \in [t_k, t_{k+N}) \tag{6d}$$

$$\hat{V}(\hat{x}(t)) \le \hat{\rho}_{ei}, \forall\ t \in [t_k, t_{k+N}) \quad \text{if} \quad x(t_k) \in \Omega_{\hat{\rho}_{ei}} \tag{6e}$$

$$\frac{\partial \hat{V}(x(t_k))}{\partial x}(A_i x(t_k) + B_i u(t_k)) \le \frac{\partial \hat{V}(x(t_k))}{\partial x}(A_i x(t_k) + B_i h_{Li}(x(t_k))) \quad \text{if} \quad x(t_k) \notin \Omega_{\hat{\rho}_{ei}} \tag{6f}$$

where the notation follows that in eq 5, and $\hat{x}(t)$ denotes the state prediction using the linear empirical model (eq 6b), starting from the state feedback measurement (eq 6c). The subsets of the stability regions for the Mode 1 constraints $\Omega_{\hat{\rho}_{ei}} \subset \Omega_{\hat{\rho}_i}$ are chosen

DOI: 10.1021/acs.iecr.7b00576
Ind. Eng. Chem. Res. 2017, 56, 5652−5667

to make the stability region $\Omega_{\hat{\rho}_i}$ forward invariant in the presence of bounded process disturbances. Both $\Omega_{\hat{\rho}_i}$ and $\Omega_{\hat{\rho}_{ei}}$ that make $\Omega_{\hat{\rho}_i}$ forward invariant can be difficult to determine in practice. Therefore, a conservative estimate of each can be chosen, or they can be adjusted online based on analyzing the process data to determine whether the LEMPC of eq 6 is able to maintain the state within an expected region of state-space.

Moving Horizon Error Detector. In this section, we describe the moving horizon error detector that quantifies prediction errors and triggers online model identification when necessary. Specifically, the moving horizon error detector tracks an error metric throughout the duration of process operation that is based on the difference between the predicted states using a linear empirical model and the measured states from the process (relative prediction error). When this error exceeds an engineer-specified threshold $e_{d,T}$ (indicating significant plant/model mismatch), online model reidentification is triggered and performed using the most recent input/output data points, and the updated model is used in the LEMPC of eq 6. The error metric e_d calculated by the moving horizon error detector at each sampling time t_k using the most recent past state predictions and measurements in a moving horizon fashion is presented in the following equation:

$$e_d(t_k) = \sum_{r=0}^{M} \sum_{j=1}^{n} \frac{|x_{p,j}(t_{k-r}) - x_j(t_{k-r})|}{|x_j(t_{k-r})|} \tag{7}$$

where the horizon M is the number of sampling periods included in assessing the prediction error. $x_j(t_{k-r})$ and $x_{p,j}(t_{k-r})$, $r = 0, ..., M$, $j = 1, ..., n$, are the past process state measurements and the past state predictions from an empirical model between the sampling times t_{k-M} and t_k. Due to the fact that process states may vary in their orders of magnitude, the difference between the predicted states and the measured states is normalized by the magnitude of the measured state $|x_j(t_{k-r})|$. The purpose of summing over the horizon M is to average out the effect of small time-varying disturbances that may occur in practice and cause prediction errors to increase. For the detailed guidelines and the step-by-step procedure for determining the values of the horizon M and the error metric threshold $e_{d,T}$ for a given process, the reader may refer to ref 24.

Implementation Strategy. In this section, we present the steps taken in the proposed online model identification scheme to overcome actuator faults in empirical model-based LEMPC as follows:

Step 1. Before an actuator fault occurs, an initial linear empirical model (A_1 and B_1) accounting for all actuators is obtained by exciting the system with a large number of inputs that have varying magnitudes and collecting the corresponding output data. This model is used to predict the process evolution within the LEMPC and to design the stabilizing controller h_{L1} and the corresponding $\hat{V}$ for the Lyapunov-based constraints of the LEMPC. The region $\Omega_{\hat{\rho}_{ei}}$ is chosen such that, in this region, plant−model mismatch is minimal.

Step 2. The process is operated under the LEMPC design using an empirical model, and the moving horizon error detector is used to detect prediction errors.

Step 3. When an actuator fault occurs, the LEMPC receives information on which actuator is stuck. If the value at which the actuator is stuck is known, the corresponding input value in the LEMPC optimization problem is fixed to the fault value and the decision variables for this input are removed from the LEMPC optimization problem (i.e., the LEMPC no longer solves for the input corresponding to the faulty actuator). If the value at which the actuator is stuck is unknown, the LEMPC optimization problem continues to compute optimal control actions for all actuators (assuming that all actuators are active online) despite the fact that a fault has occurred in one of them (i.e., the LEMPC solves for all the inputs including the input corresponding to the faulty actuator despite the fact that it will not be implemented since this actuator is not under control).

Step 4. If $e_d(t_k)$ exceeds $e_{d,T}$, input and output data collected since the fault occurrence are used to identify a new model online for use in the LEMPC formulation and the design of the corresponding stabilizing controller h_{Li}. The new B_i matrix obtained will contain one less column since the number of manipulated inputs is reduced by one.

Step 5. Process operation under the LEMPC and the moving horizon error detector continues (i.e., return to Step 2 and proceed to Steps 3 through 5 if another actuator fault occurs).

Remark 1. This work focuses on economic model predictive control (EMPC), which may operate a process in a dynamic or time-varying fashion because, as shown in eqs 5 and 6, it attempts to minimize a general objective function, subject to constraints, by choosing appropriate control actions throughout the prediction horizon. This general objective function would often not have its minimum at a process steady-state, and therefore, the process is not necessarily operated at steady-state because the EMPC may compute inputs with a periodic trajectory or a time-varying trajectory that is not periodic. A dynamic operating policy has been shown to be economically beneficial compared to steady-state operation for a number of processes (e.g., ethylene oxidation in a continuous stirred tank reactor[25] and parallel reactions in a continuous stirred tank reactor[26]). In the case that EMPC computes a time-varying input policy, the inputs may be persistently exciting and thus may allow a sufficiently accurate model to be obtained from routine process operating data. The expected input trajectories of an EMPC for a given process (with various inputs online and faulty) should be evaluated before the error-triggered online model identification procedure for fault-tolerant control is implemented to ensure that, under normal operating conditions and also as actuators experience faults, the inputs expected during routine process operation will be persistently exciting. In the case that they are, the time-varying input trajectories that may be generated under EMPC may make the input/output data convenient for use in online model identification.

Remark 2. Conditions guaranteeing feasibility and closed-loop stability of an LEMPC based on a linear empirical model that is not updated in time have been developed in ref 15. These conditions include requirements that the empirical model must be sufficiently close to the linearization of the underlying nonlinear model. In the proposed methodology, when an actuator fault occurs, the underlying nonlinear model changes, but the process model cannot be immediately updated because no postfault process input/output data is available. Therefore, it is not possible to assess if the previous linear empirical model is close to the linearization of the underlying nonlinear model after the fault has occurred, regardless of whether the value of the fault is known and it is fixed in the empirical model or the value of the fault is unknown and the empirical model is used assuming all inputs are active online. Due to this practical difficulty, proving guaranteed feasibility and closed-loop stability of the error-triggered online model identification for LEMPC scheme has not been pursued. As a result, selecting $\hat{V}$, $\Omega_{\hat{\rho}_i}$, $\Omega_{\hat{\rho}_{ei}}$, and h_{Li} to provide

DOI: 10.1021/acs.iecr.7b00576
Ind. Eng. Chem. Res. 2017, 56, 5652−5667

guaranteed closed-loop stability of the nonlinear process when used in the LEMPC can be challenging. However, appropriate parameters can be determined practically using closed-loop simulations with the linear empirical model in the LEMPC when a first-principles model is available for analyzing the accuracy of the state predictions and the ability of the LEMPC with an empirical model to maintain closed-loop stability of the nonlinear process, and then some conservatism can be added to the estimates of the parameters. Alternatively, conservative estimates of $\Omega_{\hat{\rho}_i}$ and $\Omega_{\hat{\rho}_{ei}}$ can be utilized initially when a first-principles model is not available, and updated online if desired to reduce the conservatism after process operating data is available. In general, because process data is monitored frequently, the parameters can be tuned online if the closed-loop performance does not meet an engineer's expectations. Therefore, the lack of a rigorous closed-loop stability and feasibility proof for this LEMPC design does not pose practical limitations and it would be expected to be effective in many practical applications.

Remark 3. The moving horizon error detector is also capable of initiating empirical model updates when significant plant variations, operating region changes, or disturbances that are not caused by actuator faults occur,[24] and it may also trigger model reidentification multiple times after a fault if the reidentified models were developed without sufficient postfault input/output data to allow the model to adequately capture the postfault process dynamics. When significant plant variations or disturbances or poorly identified postfault models cause the prediction error to exceed the predefined threshold for the error metric $e_d(t_k)$, the same steps mentioned above are taken excluding Step 3 and the dimension of the updated B_i matrix remains the same as the B_i from the previous linear empirical model. Furthermore, any known and sudden disturbance that does not correspond to loss of a new actuator but which may change the underlying process dynamics (e.g., an actuator that has already become stuck at one value becomes stuck at another value due to a disturbance that affects the actuator position, or an on−off aspect of the process such as a pump or valve that is not manipulated by the control system has been changed) can also be handled with the implementation strategy detailed in this section (e.g., only data corresponding to the time after the known disturbance may be used in the model reidentification due to the change in the underlying process dynamics), except that the number of columns in the B_i matrix would not change if the disturbance did not affect the number of online actuators compared to the previous model reidentification. In practice, when an unknown disturbance or plant variation occurs and causes the prediction error to exceed the predefined threshold for the error metric $e_d(t_k)$, the time at which this unknown disturbance or plant variation started may also be unknown. Therefore, the number of input/output data points N_d utilized in each model identification after the threshold for the error metric $e_d(t_k)$ has been exceeded remains the same as the number utilized for obtaining the initial model (A_1 and B_1) since no extra information is available. If the reidentified model was developed without sufficient input/output data collected after the occurrence of the disturbance or plant variation, the threshold for the error metric $e_d(t_k)$ may be exceeded multiple times until enough input/output data collected after the occurrence of the disturbance or plant variation are available and the resulting identified model adequately captures the process dynamics. The ability of the moving horizon error detector to handle the many scenaria discussed in this remark, even simultaneously, makes it an integrated approach to handling a variety of practical considerations.

Remark 4. In ref 24, guidelines for determining M, $e_{d,T}$, and the number of input/output data points to utilize in model reidentification were presented assuming that the causes of plant/model mismatch are gradual changes such as plant variations, disturbances, or movement of the process state into new regions not captured by the original linear empirical model throughout time. However, actuator faults occur suddenly, which may cause an identified empirical model to rapidly become inadequate for representing the process dynamics. Therefore, process data and controller performance should be monitored after the fault to ensure that M, $e_{d,T}$, and the number of process data points chosen for model reidentification, determined using the nonfaulty plant operating data and methods like those in ref 24, remain valid for assessing the prediction error and obtaining sufficiently accurate models upon reidentification after the fault. If they do not, as in ref 24, the values of M and $e_{d,T}$ can be increased or decreased online and the effect of this on the controller performance can be examined to arrive at updated values of M and $e_{d,T}$ when required. Furthermore, the last M data points including nonfaulty data may continue to be used in evaluating the prediction error after the fault (due to the inability to set an error threshold on fewer than M postfault data points alone after the fault since there would be no basis for the alternative error threshold, and the fact that very large prediction errors in the postfault data will still trigger model reidentification if necessary before M postfault data points are available even if prefault data is also included in the calculation of e_d). Similarly, when sufficient input/output data points are available after the fault for use for model reidentification, this number of data points can be increased or decreased based on controller performance to ensure that it is still satisfactory after the fault. If the number of input/output data points N_d used for model reidentification before the fault is greater than the number of postfault input/output data points available after the fault when model reidentification is first triggered by the moving horizon error detector, then only the postfault data (i.e., less than the desired N_d) should be used for the reidentification. This is because the input/output model structure changes after the fault (i.e., there is one less input), with the result that the data corresponding to having one additional input from before the fault cannot be used in identifying a model corresponding to having one less input from after the fault. If a sufficiently accurate model is not identified due to the lack of sufficient postfault data when the moving horizon error detector is triggered, it would be expected that the prediction error will eventually increase once again above $e_{d,T}$, triggering another model reidentification with additional postfault data, so that eventually the linear empirical model used after the fault will have been developed with sufficient postfault input/output data to allow for sufficiently accurate state predictions that no longer trigger model reidentification.

Remark 5. Though the error-triggered model update strategy for actuator fault compensation is discussed in the context of LEMPC, it can be extended to other model-based control designs, including tracking MPC (MPC with a quadratic objective function), as well, as long as the process data available for updating the models when these other control designs are used contains enough information regarding the important process dynamics for use in identifying sufficiently accurate process models.

Remark 6. It was previously noted that multiple simultaneous faults as well as actuator recommissioning can be handled

DOI: 10.1021/acs.iecr.7b00576
Ind. Eng. Chem. Res. 2017, 56, 5652−5667

utilizing this strategy. The simultaneous faults may include those for which the value of the faulty actuator output is known, those for which it is unknown, or even a combination. For multiple simultaneous faults, Step 3 is applied to the various faulty actuators, and in Step 4, the number of columns in the B_i matrix is reduced by the number of faulty actuators. For actuator recommissioning, model reidentification using the most recent N_d input/output data points since the last actuator fault (or the total number available since the last fault if the available number is less than N_d) can be performed, allowing the B_i matrix to include columns for all actuators that are now nonfaulty. This model can then be utilized in the LEMPC, and the error-triggering procedure will update the model if the state predictions contain significant error due to the fact that the input/output data on which the model was based did not include the effects of the recommissioned actuators taking output values different from the value at which they were stuck.

Remark 7. When the value at which a faulty actuator is stuck is unknown, other methods of accounting for this faulty actuator in the empirical model immediately after the fault could be utilized instead of continuing to solve for all actuator outputs as suggested in Step 3. The goal of Step 3 when the actuator output is unknown is to allow the LEMPC to continue computing control actions for the nonfaulty actuators while generating input/output data that can be used to identify a model corresponding to the process dynamics subject to the fault, and this can be done with any reasonable assumption on the value of the faulty actuator outputs in the LEMPC.

Remark 8. The approach presented can be extended to the case that nonlinear empirical models are utilized in place of linear empirical models. Specifically, the five steps of the implementation strategy of the error-triggered model update strategy would still be undertaken, but with a nonlinear empirical model identified and utilized to determine a Lyapunov function and Lyapunov-based controller for use in the LEMPC design. Because the objective function of an EMPC often depends on some, if not all, of the process states, a state-space nonlinear empirical model is most desirable for use in EMPC, which can be identified using techniques such as those in refs 27 and 28. However, the computation time required to solve a nonlinear empirical model within a sampling period may be longer than that required to solve a linear empirical model, particularly since no analytic solution exists in general for a nonlinear system (and thus numerical integration techniques are required to solve the empirical model), whereas the availability of the analytic solution of a linear empirical model may aid in reducing computation time compared to numerically integrating the linear system. Due to the potential computation time benefits of utilizing a linear empirical model compared to utilizing a nonlinear empirical model, this work has focused on model identification and reidentification with linear models that can be updated via the error-triggering procedure discussed in this work when the process state moves into regions where the process nonlinearities are no longer captured by the original linear empirical model.[24]

Remark 9. Though the approach could be considered in the case that stochastic models are identified from process data instead of deterministic models, we focus on identifying deterministic models in this work due to the difficulty of implementing EMPC with stochastic models (which often leads to high computation times due to the need to solve the dynamic process model under many realizations of the disturbance vector to calculate quantities such as expectations of the objective function or of quantities in the constraints). Standard techniques for data smoothing/filtering should be employed during the model identification procedure to obtain an accurate process model.

Remark 10. Because EMPC utilizes a general objective function, the objective function may depend on process states. As a result, we utilize state-space empirical models in this work and assume that measurements are available for, at a minimum, all states that appear in the objective function (or the constraints). The empirical model order thus is assumed to be no less than the order of the corresponding first-principles model that includes all process states that enter the EMPC cost and constraints. The notation in the section Class of Systems assumes that the number of states in the first-principles model for the system is equal to the number of states in the empirical model, though this is an assumption that could be relaxed when designing EMPC with error-triggered online model identification, as long as the requirements in this remark are met by the empirical model.

APPLICATION OF ERROR-TRIGGERED ONLINE MODEL IDENTIFICATION WHEN THE FAULT VALUE IS KNOWN: CATALYTIC PROCESS EXAMPLE

This section demonstrates the application of the proposed error-triggered online model identification procedure for fault-tolerant LEMPC when the value at which the actuator is stuck is known. We consider the control of catalytic oxidation of ethylene (C_2H_4) in a continuous stirred tank reactor (CSTR). Ethylene is oxidized with air to produce the desired ethylene oxide (C_2H_4O) product as presented in the following chemical reactions:

$$C_2H_4 + \frac{1}{2}O_2 \xrightarrow{R_1} C_2H_4O \quad \text{(R1)}$$

$$C_2H_4 + 3O_2 \xrightarrow{R_2} 2CO_2 + 2H_2O \quad \text{(R2)}$$

$$C_2H_4O + \frac{5}{2}O_2 \xrightarrow{R_3} 2CO_2 + 2H_2O \quad \text{(R3)}$$

The reaction rates R_1, R_2, and R_3 are given by the following Arrhenius relationships:[29]

$$R_1 = k_1 \exp\left(\frac{-E_1}{R_g T}\right) {P_E}^{0.5} \quad \text{(8a)}$$

$$R_2 = k_2 \exp\left(\frac{-E_2}{R_g T}\right) {P_E}^{0.25} \quad \text{(8b)}$$

$$R_3 = k_3 \exp\left(\frac{-E_3}{R_g T}\right) {P_{EO}}^{0.5} \quad \text{(8c)}$$

where k_1, k_2, and k_3 are pre-exponential factors, E_1, E_2, and E_3 are activation energies for each reaction, R_g is the gas constant, and T is the absolute temperature. The reaction rates are presented in terms of partial pressures of ethylene (P_E) and of ethylene oxide (P_{EO}). The gas mixture inside the reactor is assumed to be ideal, and thus, the partial pressures in the reaction rates can be converted to molar concentrations using the ideal gas law. The dimensionless mass and energy balances for this process are described by the following first-order ordinary differential equations:[25]

$$\frac{dx_1(t)}{dt} = u_1(1 - x_1 x_4) \quad \text{(9a)}$$

DOI: 10.1021/acs.iecr.7b00576
Ind. Eng. Chem. Res. 2017, 56, 5652−5667

$$\frac{dx_2(t)}{dt} = u_1(u_2 - x_2x_4) - A_1\, e^{\gamma_1/x_4}(x_2x_4)^{0.5} - A_2\, e^{\gamma_2/x_4}(x_2x_4)^{0.25} \quad (9b)$$

$$\frac{dx_3(t)}{dt} = -u_1x_3x_4 + A_1\, e^{\gamma_1/x_4}(x_2x_4)^{0.5} - A_3\, e^{\gamma_3/x_4}(x_3x_4)^{0.5} \quad (9c)$$

$$\frac{dx_4(t)}{dt} = \frac{u_1}{x_1}(1 - x_4) + \frac{B_1}{x_1}e^{\gamma_1/x_4}(x_2x_4)^{0.5} + \frac{B_2}{x_1}e^{\gamma_2/x_4}(x_2x_4)^{0.25} + \frac{B_3}{x_1}e^{\gamma_3/x_4}(x_3x_4)^{0.5} - \frac{B_4}{x_1}(x_4 - u_3) \quad (9d)$$

where x_1, x_2, x_3, and x_4 are the dimensionless gas density, ethylene concentration, ethylene oxide concentration, and temperature inside the reactor, respectively. The reactor manipulated inputs are the dimensionless volumetric flow rate of the inlet stream u_1, the dimensionless concentration of ethylene in the inlet stream u_2, and the dimensionless coolant temperature u_3. The manipulated inputs are constrained to belong to the following sets: $0.0704 \le u_1 \le 0.7042$, $0.2465 \le u_2 \le 2.4648$, $0.6 \le u_3 \le 1.1$. Table 1 lists the values of the process parameters. The reactor has an asymptotically stable steady-state at $[x_{1s}\ x_{2s}\ x_{3s}\ x_{4s}] = [0.998\ 0.424\ 0.032\ 1.002]$ corresponding to the manipulated input values of $[u_{1s}\ u_{2s}\ u_{3s}] = [0.35\ 0.5\ 1.0]$.

Table 1. Dimensionless Parameters of the Ethylene Oxidation CSTR

$A_1 = 92.8$	$B_2 = 10.39$	$\gamma_2 = -7.12$
$A_2 = 12.66$	$B_3 = 2170.57$	$\gamma_3 = -11.07$
$A_3 = 2412.71$	$B_4 = 7.02$	
$B_1 = 7.32$	$\gamma_1 = -8.13$	

The control objective is to maximize the average yield of ethylene oxide by operating the reactor in a time-varying manner around the open-loop stable steady-state. Over a time period from t_0 to t_e, this average yield is given by

$$Y(t_e) = \frac{\int_{t_0}^{t_e} u_1(\tau)\, x_3(\tau)\, x_4(\tau)\, d\tau}{\int_{t_0}^{t_e} u_1(\tau)\, u_2(\tau)\, d\tau} \quad (10)$$

t_e is an integer multiple of t_f which is the length of an operating period. In addition, we consider that there is a limitation on the amount of ethylene that may be fed to the rector during the length of an operating period t_f. Therefore, the time-averaged amount of ethylene that can be fed to the reactor should satisfy the following material constraint:

$$\frac{1}{t_f}\int_{(j-1)t_f}^{jt_f} u_1(\tau)\, u_2(\tau)\, d\tau = u_{1s}u_{2s} = 0.175 \quad (11)$$

where j is the operating period number ($j = 1, 2, \ldots$). Since the material constraint of eq 11 fixes the average amount of ethylene fed to the reactor over the operating period t_f, the economic cost that the LEMPC attempts to maximize such that the ethylene oxide yield is maximized becomes

$$\int_{t_0}^{t_e} L_e(x, u) = \int_{t_0}^{t_e} u_1(\tau)\, x_3(\tau)\, x_4(\tau)\, d\tau \quad (12)$$

We assume that the reactor first-principles model in eq 9 is unavailable for control design. Therefore, an empirical model is used to design the LEMPC with the objective function and constraints mentioned above. To construct an empirical model that captures the process dynamics accurately in a region local to the stable steady-state, a large sequence of step inputs with varying magnitudes was applied to the reactor in order to excite the important dynamics and capture them in the empirical model. After collecting the input/output data points, the initial ($i = 1$) state-space linear empirical model of the reactor was obtained using the ordinary multivariable output error state-space (MOESP)[8] algorithm. Model validation was then conducted using various step, impulse, and sinusoidal input responses. The initial empirical model obtained is given by the following constant matrices:

$$A_1 = \begin{bmatrix} -0.349 & 0.00051 & 0.00825 & -0.349 \\ -0.00488 & -0.374 & 0.0374 & -0.369 \\ 0.00109 & 0.0213 & -0.452 & 0.0653 \\ -0.0078 & 0.0259 & 0.0204 & -7.24 \end{bmatrix},$$

$$B_1 = \begin{bmatrix} -0.00011 & -0.000149 & -0.0239 \\ 0.0757 & 0.349 & -0.0194 \\ -0.0315 & 0.000208 & 0.00426 \\ -0.0173 & -0.00264 & 6.529 \end{bmatrix} \quad (13)$$

The stabilizing control law used in the LEMPC is designed based on the empirical model of eq 13 since we assumed that the reactor first-principles model of eq 9 is unavailable. The stabilizing control law is represented by the three-dimensional vector $h_{L1}^T(x) = [h_{L1,1}(x)\ h_{L1,2}(x)\ h_{L1,3}(x)]$. In order to meet the material constraint of eq 11 on the available feedstock, both $h_{L1,1}(x)$ and $h_{L1,2}(x)$ were set to their steady-state values. The linear quadratic regulator (LQR) was used in designing the third control law $h_{L1,3}(x)$ using the A_1 matrix and the third column of the B_1 matrix as the system matrices. Both LQR weighting matrices Q and R were taken to be the identity matrix. The resulting control law for the heat input is $u_3 = h_{L1,3}(x) = -K(x - x_s) + u_{3s}$, with K equal to $[-0.287\ -0.276\ 0.023\ 0.405]$. The closed-loop stability region is characterized using the quadratic Lyapunov function $\hat{V}(x) = (x - x_s)^T P(x - x_s)$ where the positive definite matrix P is $P = \mathrm{diag}[20\ 30\ 40\ 10]$. Through extensive closed-loop simulations of the reactor system under the stabilizing control law $h_{L1}(x)$, the level sets $\Omega_{\hat{\rho}_1}$ and $\Omega_{\hat{\rho}_{e1}}$ were chosen to have $\hat{\rho}_1 = 96.1$ and $\hat{\rho}_{e1} = 87.4$. In these regions, the reactor first-principles nonlinear dynamics of eq 9 are well-captured by the linear empirical model of eq 13.

To compare the closed-loop performance of the process even in the presence of actuator faults when an LEMPC based on a linear empirical model is used instead of an LEMPC based on the first-principles model, two LEMPC schemes, one of the form of eq 6 and the other of the form of eq 5, were designed for the CSTR with the cost function of eq 12 and the material constraint of eq 11 to compare closed-loop behavior. The first LEMPC initially utilized the model of eq 13 to predict the values of the process states throughout the prediction horizon, while the second LEMPC utilized the first-principles model of eq 9 (though both used the same Lyapunov-based controller and stability region). All LEMPC designs presented in this chemical process example use a prediction horizon of $N = 10$, a sampling period of $\Delta = 0.1$, and an operating period of 100 sampling periods ($t_f = 10$). The open-source optimization solver IPOPT[30] was used in solving the LEMPC optimization problems at each

DOI: 10.1021/acs.iecr.7b00576
Ind. Eng. Chem. Res. 2017, 56, 5652−5667

sampling time. The empirical LEMPC and the first-principles LEMPC were both applied to the CSTR model of eq 9. Closed-loop simulations of the reactor under each LEMPC design were performed starting from the open-loop stable steady-state $x_I^T = [x_{1I}\ x_{2I}\ x_{3I}\ x_{4I}] = [0.997\ 1.264\ 0.209\ 1.004]$. Simulations were performed using the Explicit Euler numerical integration method with an integration step size of $h = 10^{-4}$.

In order to demonstrate the effect of actuator faults on controlling the process using empirical models and the need to reidentify a new model online after a fault occurs, the reactor was simulated for four operating periods under the empirical LEMPC design. After three operating periods, an actuator fault is assumed to occur causing the heat input to stay at the steady-state value (i.e., $u_3 = 1$). After that, the reactor was operated in closed-loop using the empirical LEMPC design with u_3 set to its steady-state value in the empirical model defined by A_1 and B_1 (eq 13). For comparison, the closed-loop state and input trajectories were simulated for the first-principles LEMPC, including u_3 set to its steady-state value after three operating periods in the first-principles model for the LEMPC. For the first three operating periods (i.e., before the fault), the empirical and first-principles LEMPC's compute very similar input trajectories resulting in similar closed-loop state trajectories under both controllers, as shown in Figures 1 and 2. This indicates that, before the fault, the

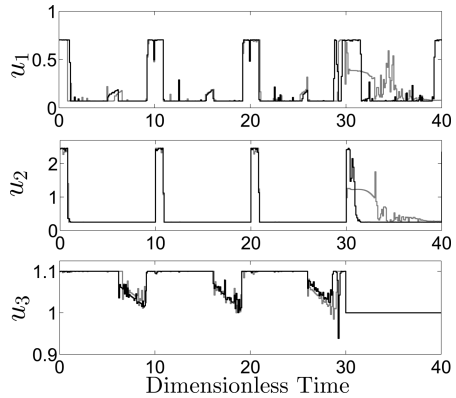

Figure 1. Closed-loop input trajectories for four operating periods of the reactor of eq 9 initiated from x_I under the LEMPC designed with the first-principles model (solid black trajectories) and the LEMPC designed with the empirical model in eq 13 (solid gray trajectories) where an actuator fault occurs at the end of the 3rd operating period.

LEMPC with an empirical model is an effective control design for the reactor process (it is noted that u_1, u_2, and u_3 in Figure 1 correspond to the inputs calculated by the LEMPC's, rather than the input trajectories computed by the Lyapunov-based controller h_{L1} that is used in the design of the LEMPC constraints; therefore, the trajectories of u_1, u_2, and u_3 in the figure are those that the LEMPC's determined would optimize the objective function subject to the constraints). The reactor input and state trajectories under both the empirical and first-principles LEMPC's when $u_3 = u_{3s}$ after the first three operating periods are also depicted in Figures 1 and 2, and they exhibit significant differences, indicating significant plant−model mismatch and resulting in less yield of the final desired product under the empirical LEMPC. This demonstrates the need to reidentify the model online.

Based on the above simulations, it is expected that the closed-loop performance of the ethylene oxide production process under LEMPC with an empirical model would benefit from the

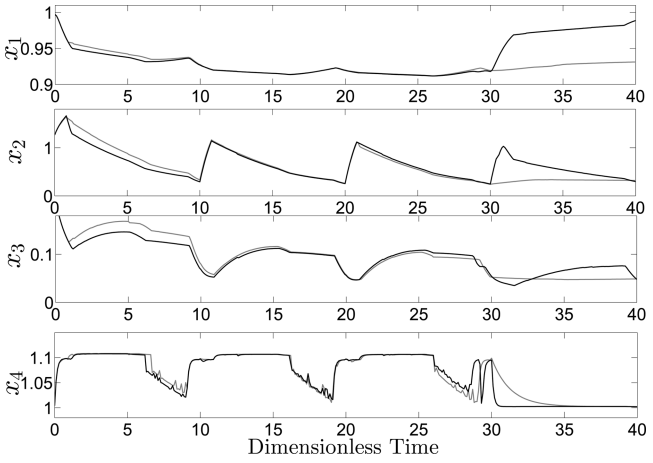

Figure 2. Closed-loop state trajectories for four operating periods of the reactor of eq 9 initiated from x_I under the LEMPC designed with the first-principles model (solid black trajectories) and the LEMPC designed with the empirical model in eq 13 (solid gray trajectories) where an actuator fault occurs at the end of the 3rd operating period.

use of the error-triggered online model identification procedure after a process fault. Therefore, simulations of the ethylene oxide process under the implementation strategy presented in this work were performed. Specifically, a moving horizon error detector was designed and initiated after $M = 40$ input/output data points were available to calculate the value of e_d at each sampling time to determine when it is necessary to trigger reidentification of the empirical process model. Simulations of the reactor suggested that significant plant−model mismatch was indicated when the value of e_d exceeded 3, and thus, this value was chosen as the threshold to trigger model reidentification. When online model identification was triggered, input/output data collected after the occurrence of the fault was used to identify a new model. The moving horizon error detector calculates the relative prediction error in the gas density in the reactor, ethylene concentration, ethylene oxide concentration, and the reactor temperature throughout the current and past 40 sampling periods as follows:

$$e_d(t_k) = \sum_{r=0}^{40} \left[\frac{|x_{1_p}(t_{k-r}) - x_1(t_{k-r})|}{|x_1(t_{k-r})|} + \frac{|x_{2_p}(t_{k-r}) - x_2(t_{k-r})|}{|x_2(t_{k-r})|} + \frac{|x_{3_p}(t_{k-r}) - x_3(t_{k-r})|}{|x_3(t_{k-r})|} + \frac{|x_{4_p}(t_{k-r}) - x_4(t_{k-r})|}{|x_4(t_{k-r})|} \right] \tag{14}$$

The initial empirical model utilized within the LEMPC coupled with the moving horizon error detector/online model reidentification strategy was again A_1 and B_1, and the reactor was again initiated from x_I. As in the above simulation, after three operating periods (i.e., at the beginning of the 4th operating period), an actuator fault occurs, causing the heat input to stay at the steady-state value (i.e., $u_3 = 1$) for three operating periods. The LEMPC was apprised of the fault in the actuator corresponding to u_3, and the value of u_3 in the linear empirical model utilizing the A_1 and B_1 matrices was subsequently set to the value u_{3s} at which it was stuck. The first six operating periods depicted in Figure 3 show the increase in e_d after the fault occurrence, leading it to eventually exceed its threshold and trigger online model reidentification that resulted in a sharp drop

DOI: 10.1021/acs.iecr.7b00576
Ind. Eng. Chem. Res. 2017, 56, 5652−5667

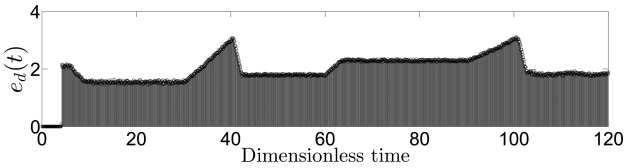

Figure 3. Value of error metric e_d at each sampling time using the detector of eq 14 for the LEMPC integrated with the error-triggered online model identification.

in the prediction error. The following model was identified using the postfault input/output data:

$$A_2 = \begin{bmatrix} -149.8 & -1.30 & -6.71 & -0.347 \\ -2276 & 20.3 & 72.9 & -0.235 \\ 1469 & -13.4 & -59.8 & 0.0220 \\ -120.3 & -1.10 & 14.2 & -7.31 \end{bmatrix},$$

$$B_2 = \begin{bmatrix} -0.0021 & -0.004 \\ 0.0454 & 0.202 \\ 0.0018 & 0.062 \\ 0.0188 & 0.008 \end{bmatrix} \quad (15)$$

Notably, in accordance with Step 4 of the implementation strategy presented in this work, the B_2 matrix has one less column than the B_1 matrix due to the loss of availability of u_3 as a manipulated input.

It was noted in Remark 3 that the error-triggered online model reidentification procedure can be used not only for handling actuator faults but also for handling other disturbances and plant variations, even sudden changes in the process dynamics that do not affect the number of online actuators. Therefore, the error-triggered online model reidentification procedure for use in LEMPC provides a unified framework for dealing with many different root causes of reduced accuracy of state predictions from linear empirical models. To demonstrate how this unified framework can be implemented, we followed the six operating periods related to the process fault discussed above with six more operating periods (for a total simulation length of 12 operating periods) in which the actuator u_3 remained stuck (i.e., unavailable as a manipulated input by the LEMPC), but we assumed that it was subjected to disturbances that caused it to take two other known values throughout these six operating periods (e.g., a valve utilized in setting u_3 experienced a large degree of stiction but slipped to two new values due to changes in the forces applied to it twice throughout the six operating periods). Specifically, the value of u_3 changed to its maximum value of 1.1 at the beginning of the 7th operating period and remained stuck at this value for three operating periods, and then it changed to the value of 0.75 at the beginning of the 10th operating period and remained stuck at this value for another three operating periods. Throughout the six operating periods during which the value of u_3 experienced these disturbances, only one model reidentification was triggered by the moving horizon error detector, leading to a drop in the prediction error as shown in Figure 3 when the following model was identified:

$$A_3 = \begin{bmatrix} -27.39 & 15.4 & 7.29 & -25.8 \\ 33.39 & -18.2 & 12.3 & 30.14 \\ -16.95 & -4.20 & -201 & 2.004 \\ -168.1 & 87.1 & -26.4 & -155.9 \end{bmatrix},$$

$$B_3 = \begin{bmatrix} 0.1771 & -0.541 \\ 0.2206 & -0.260 \\ -0.018 & 0.0397 \\ -0.203 & 0.8383 \end{bmatrix} \quad (16)$$

This model reidentification was triggered when $u_3 = 0.75$ (i.e., no model reidentification was triggered when $u_3 = 1.1$), showing that the error-triggering was successful at deciding the necessity of model updates, because even though u_3 changed its value at the beginning of the 7th operating period, no reidentification was required since the error did not exceed the threshold of $e_d = 3$. Because this model reidentification was not related to loss of a new actuator, B_3 has the same dimension as B_2.

The input and state trajectories for the entire 12 operating periods of the reactor process of eq 9 under the LEMPC of eq 6 with the empirical models of eqs 13, 15, and 16 subject to the actuator fault and disturbances in the value at which u_3 was stuck are presented in Figures 4 and 5. The values of e_d throughout the

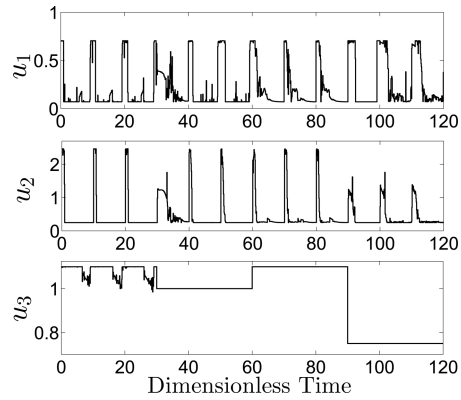

Figure 4. Closed-loop input trajectories of the reactor of eq 9 under the LEMPC using the error-triggered online model identification starting from $x_I^T = [x_{1I}\ x_{2I}\ x_{3I}\ x_{4I}] = [0.997\ 1.264\ 0.209\ 1.004]$.

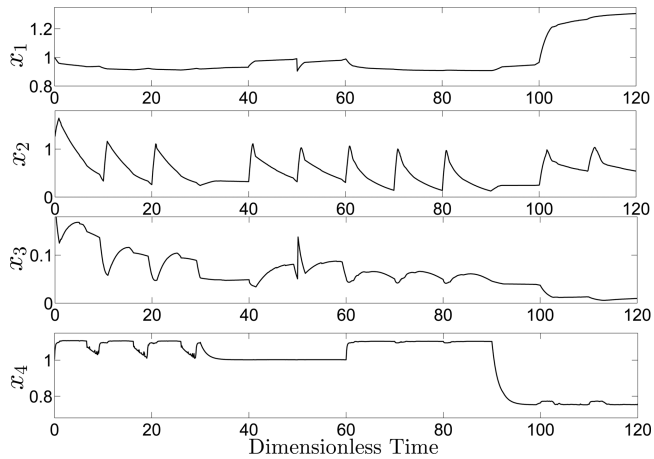

Figure 5. Closed-loop state trajectories of the reactor of eq 9 under the LEMPC using the error-triggered online model identification starting from $x_I^T = [x_{1I}\ x_{2I}\ x_{3I}\ x_{4I}] = [0.997\ 1.264\ 0.209\ 1.004]$.

DOI: 10.1021/acs.iecr.7b00576
Ind. Eng. Chem. Res. 2017, 56, 5652−5667

12 operating periods is presented in Figure 3, showing the rises of the e_d values that triggered the model reidentifications and the rapid decreases of the values of $e_d(t_k)$ after each online model reidentification. These figures show the successful implementation of a unified framework using the moving horizon error detector and error-triggered model updates within LEMPC for handling both faults and other disturbances throughout time.

In addition to decreasing the plant−model mismatch due to faults and disturbances, the online model identification improved the process economic performance compared to not updating the model as presented in Table 2. The table lists the average yield and the maximum value of $e_d(t_k)$ for the two operating periods after the first online model reidentification (when u_3 is stuck at the value of 1) and after the second model identification (when u_3 is stuck at the value of 0.75). The results listed are for three approaches: the "One Empirical Model" approach, in which no model reidentification is conducted and the initial empirical model (A_1 and B_1) is used throughout the 12 operating periods despite the faults, the "Online Model ID" approach, in which the proposed online model reidentification approach is conducted, and the "Nonlinear Model" approach, in which the first-principles model of eq 9 is used in the LEMPC including the changes in u_3. These results show the significant improvement in process yield resulting from updating the empirical model online compared to using the same initial empirical model throughout process operation despite the faults.

Table 2. Relative Prediction Error and Average Yield for the CSTR under LEMPC

	after 1st online ID		after 2nd online ID	
approach	Y	max $e_d(t_k)$	Y	max $e_d(t_k)$
One Empirical Model	7.16	4.76	7.23	5.03
Online Model ID	8.31	1.98	8.21	1.82
Nonlinear Model	8.43		8.39	

Remark 11. In this example, the controller h_{L1} was not redesigned after the actuator fault as noted in Step 4 of the online model identification scheme because the closed-loop state never left $\Omega_{\hat{\rho}_{e1}}$ during the simulation. The example in the next section exemplifies the change in the Lyapunov-based control law when the fault occurs.

APPLICATION OF ERROR-TRIGGERED ONLINE MODEL IDENTIFICATION WHEN THE FAULT VALUE IS UNKNOWN: CSTR EXAMPLE

In this section, we use a chemical process example to demonstrate the application of the proposed error-triggered online model identification for fault-tolerant LEMPC when the value at which the actuator is stuck is unknown. The example is a non-isothermal, well-mixed continuous stirred tank reactor (CSTR) in which an irreversible second-order exothermic reaction takes place converting the reactant A to the desired product B. An inert solvent containing the reactant A with a concentration C_{A0} is fed to the reactor at a feed volumetric flow rate F and a temperature T_0. The CSTR is heated/cooled by a heating jacket that supplies/removes heat at a heat rate Q. The liquid inside the CSTR is assumed to have constant heat capacity C_p, volume V, and density ρ_L. The CSTR dynamic model, derived from mass and energy balances, that describes the reactant concentration C_A and temperature T evolution with time is presented below:

$$\frac{dC_A}{dt} = \frac{F}{V}(C_{A0} - C_A) - k_0 e^{-E/R_gT} C_A^2 \quad (17a)$$

$$\frac{dT}{dt} = \frac{F}{V}(T_0 - T) - \frac{\Delta H k_0}{\rho_L C_p} e^{-E/R_gT} C_A^2 + \frac{Q}{\rho_L C_p V} \quad (17b)$$

where the parameters k_0, E, and ΔH denote the reaction pre-exponential factor, the activation energy, and the enthalpy of the reaction, respectively. The values of the process parameters are listed in Table 3. The reactor inlet concentration C_{A0} and heat supply/removal rate Q are the manipulated inputs, which are constrained by the following maximum and minimum values: $0.5 \le C_{A0} \le 7.5$ kmol/m^3 and $-5.0 \times 10^5 \le Q \le 5.0 \times 10^5$ kJ/h. The reactor is operated around the open-loop asymptotically stable steady-state $[C_{As}\ T_s] = [1.2$ kmol/m^3 438.0 K$]$, which corresponds to the input values $[C_{A0s}\ Q_s] = [4.0$ kmol/m^3 0.0 kJ/h$]$. We rewrite the CSTR state and input vectors in deviation from this steady-state as $x^T = [C_A - C_{As}\ T - T_s]$ and $u^T = [C_{A0} - C_{A0s}\ Q - Q_s]$, in order to translate the origin to be the equilibrium of the unforced system. The process dynamic model of eq 17 and all empirical models in this example are numerically integrated using the explicit Euler method with an integration time step of $h_c = 10^{-4}$ h.

Table 3. Parameter Values of the CSTR

$T_0 = 300$ K	$F = 5.0$ m^3/h
$V = 1.0$ m^3	$E = 5.0 \times 10^4$ kJ/kmol
$k_0 = 8.46 \times 10^6$ m^3/(h kmol)	$\Delta H = -1.15 \times 10^4$ kJ/kmol
$C_p = 0.231$ kJ/(kg K)	$R = 8.314$ kJ/(kmol K)
$\rho_L = 1000$ kg/m^3	

The control objective is to maximize the time-averaged production rate of the desired product B (the process profit). Therefore, the production rate of B is used to design the cost function of the LEMPC and is given by

$$\int_{t_k}^{t_{k+N}} L_e(x, u)\, d\tau = \frac{1}{(t_{k+N} - t_k)} \int_{t_k}^{t_{k+N}} k_0 e^{-E/R_gT(\tau)} C_A^2(\tau)\, d\tau \quad (18)$$

We also consider that there is a limitation on the amount of reactant material that may be fed to the reactor in a given period of operation of length $t_p = 1$ h. Therefore, the inlet concentration input trajectory is restricted by the following material constraint:

$$\frac{1}{t_p} \int_0^{t_p} u_1(\tau)\, d\tau = 0.0 \text{ kmol/m}^3 \quad (19)$$

The purpose of this constraint is to limit the amount of reactant material fed to the reactor over each operating period $t_p = 1$ h to be equal to the amount that would be fed for steady-state operation.

The reactor first-principles model in eq 17 is assumed to be unavailable, with the result that an empirical model for the system must be identified to develop an LEMPC with the above objective and constraints. Therefore, a series of step inputs were generated and applied to the CSTR and the corresponding outputs were collected in order to identify a linear time-invariant state-space model that captures the process dynamics in a state-space region around the steady-state. Using these input and output data points, the ordinary multivariable output error state-space (MOESP)[8] algorithm was implemented to produce a linear empirical model for the reactor of eq 17. This initial ($i = 1$) model of the reactor is described by the following matrices:

DOI: 10.1021/acs.iecr.7b00576
Ind. Eng. Chem. Res. 2017, 56, 5652−5667

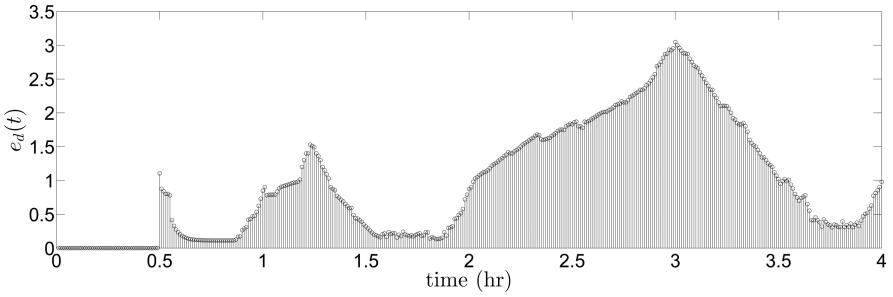

Figure 6. Value of error metric e_d at each sampling time using the detector of eq 25 for the LEMPC integrated with the error-triggered online model identification with $Q = 4.0 \times 10^4$ kJ/h after the fault.

$$A_1 = \begin{bmatrix} -34.5 & -0.473 \\ 1430 & 18.1 \end{bmatrix}, B_1 = \begin{bmatrix} 5.24 & -8.1 \times 10^{-6} \\ -11.6 & 0.457 \end{bmatrix} \tag{20}$$

Model validation was conducted using step, impulse, and sinusoidal inputs. This empirical model is used to design the Lyapunov-based controller for the LEMPC design since it is assumed that the reactor first-principles model of eq 17 is unavailable. The Lyapunov-based controller consisted of both inputs following the control law $h_{L1}^T(x) = [h_{L1,1}(x)\ h_{L1,2}(x)]$, where the reactant inlet concentration $h_{L1,1}(x)$ was fixed at 0.0 kmol/m^3 to meet the material constraint of eq 19. For the heat rate supply/removal rate, the following control law was used:[20]

$$h_{L1,2}(x) = \begin{cases} -\dfrac{L_{\tilde{f}}\hat{V} + \sqrt{L_{\tilde{f}}\hat{V}^2 + L_{g_2}\hat{V}^4}}{L_{g_2}\hat{V}}, & \text{if} \quad L_{g_2}\hat{V} \neq 0 \\ 0, & \text{if} \quad L_{g_2}\hat{V} = 0 \end{cases} \tag{21}$$

where the vector function $\tilde{f}$: $R^n \rightarrow R^n$ and the matrix function g: $R^n \rightarrow R^{n\times m}$ are defined as follows:

$$\frac{dx(t)}{dt} = \underbrace{Ax}_{=\tilde{f}(x)} + \underbrace{B}_{=g(x)}\ u \tag{22}$$

and $g_2(x)$ is the second column of the B matrix. $L_{\tilde{f}}\hat{V}$ and $L_{g_2}\hat{V}$ are the Lie derivatives of the Lyapunov function $\hat{V}(x)$ with respect to $\tilde{f}(x)$ and $g_2(x)$, respectively. A quadratic Lyapunov function of the form $\hat{V}(x) = x^T Px$ is used, where P is the following positive definite matrix:

$$P = \begin{bmatrix} 1060 & 22 \\ 22 & 0.52 \end{bmatrix} \tag{23}$$

Through extensive closed-loop simulations of the reactor system under the control law $h_{L1}(x)$, the level sets $\Omega_{\hat{\rho}_{e1}}$ and $\Omega_{\hat{\rho}_1}$ of the Lyapunov function $\hat{V}$ were chosen to have $\hat{\rho}_{e1} = 55$ and $\hat{\rho}_1 = 64.32$. In this region, the nonlinear dynamics of eq 17 are well-captured by the linear empirical model of eq 20.

In this example, the LEMPC design in eq 6 that also incorporates the material constraint of eq 19 (enforced in each operating period) is applied to the process in eq 17. We will demonstrate the case where a fault occurs in u_2. When such a fault occurs, another stabilizing control law that is based on u_1 needs to be designed to implement Mode 2 of the LEMPC if the closed-loop state exits $\Omega_{\hat{\rho}_{e1}}$. The stabilizing control law is of the following form:

$$h_{L1,1}(x) = \begin{cases} -\dfrac{L_{\tilde{f}}\hat{V} + \sqrt{L_{\tilde{f}}\hat{V}^2 + L_{g_1}\hat{V}^4}}{L_{g_1}\hat{V}}, & \text{if} \quad L_{g_1}\hat{V} \neq 0 \\ 0, & \text{if} \quad L_{g_1}\hat{V} = 0 \end{cases} \tag{24}$$

where $g_1(x)$ is the first column of the B matrix and $\hat{V}$, $\Omega_{\hat{\rho}_{e1}}$, and $\Omega_{\hat{\rho}_1}$ are the same as mentioned above. After the fault occurs, u_1 is the only manipulated input that is available both to maximize the profit and also to keep the state inside the stability region $\Omega_{\hat{\rho}_1}$, and therefore, the manipulated input trajectories calculated by the LEMPC with an empirical model may require u_1 to utilize more material than it is constrained to use by the material constraint of eq 19 (i.e., the LEMPC optimization problem may become infeasible in the second half of the operating periods after the occurrence of the fault in u_2). When the optimization problem becomes infeasible, a different optimization problem is solved to determine the value of u_1 to apply to the process, with the form of eq 6, without the material constraint of eq 19, and with the stage cost $L_e(x,u) = {u_1}^2(\tau)$ instead of the stage cost in eq 18. Mode 2 is continuously implemented so that this control design minimizes the amount of feedstock material utilized while seeking to stabilize the closed-loop system. For all of the simulations presented below, the LEMPC is designed using a prediction horizon of $N = 10$ and a sampling period of $\Delta = 0.01$ h. The open-source optimization solver IPOPT[30] was used in solving the LEMPC optimization problems at each sampling time.

The CSTR was initialized from the open-loop stable steady-state and was controlled using the LEMPC designed with the cost function of eq 18 and the material constraint of eq 19. The LEMPC utilizes the model of eq 20 to predict the values of the process states throughout the prediction horizon. A moving horizon error detector that calculates e_d at each sampling time to determine when it is necessary to trigger reidentification of the empirical process model was designed and initiated after $M = 50$ input/output data points were available. Simulations of the CSTR suggested that significant plant−model mismatch was indicated when the value of e_d exceeded 3, and thus, this value was chosen as the threshold to trigger model reidentification. The moving horizon error detector calculates the relative prediction error in the concentration and temperature throughout the past 50 sampling periods and current sampling time as follows:

$$e_d(t_k) = \sum_{r=0}^{50}\left[\frac{|T_p(t_{k-r}) - T(t_{k-r})|}{|T(t_{k-r})|} + \frac{|C_{A_p}(t_{k-r}) - C_A(t_{k-r})|}{|C_A(t_{k-r})|}\right] \tag{25}$$

DOI: 10.1021/acs.iecr.7b00576
Ind. Eng. Chem. Res. 2017, 56, 5652−5667

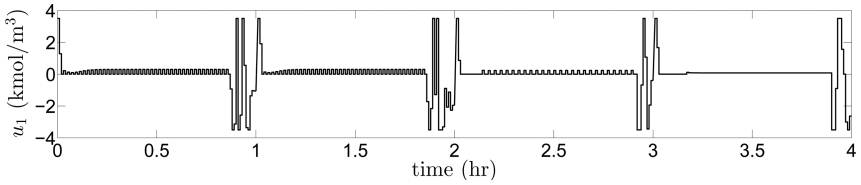

Figure 7. Closed-loop input trajectory ($u_1 = C_{A0} - C_{A0s}$) of the reactor of eq 17 under the LEMPC using the error-triggered online model identification starting from $[C_{As}\ T_s] = [1.2\ \text{kmol/m}^3\ 438.0\ \text{K}]$ with $Q = 4.0 \times 10^4$ kJ/h after the fault.

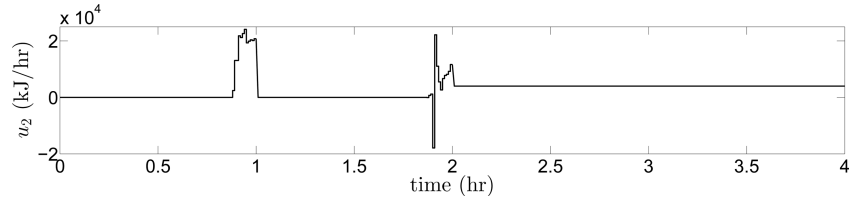

Figure 8. Closed-loop input trajectory ($u_2 = Q - Q_s$) of the reactor of eq 17 under the LEMPC using the error-triggered online model identification starting from $[C_{As}\ T_s] = [1.2\ \text{kmol/m}^3\ 438.0\ \text{K}]$ with $Q = 4.0 \times 10^4$ kJ/h after the fault.

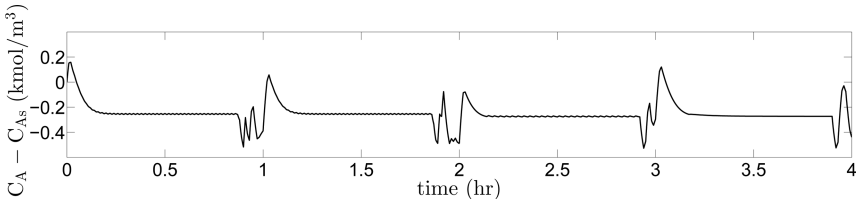

Figure 9. Closed-loop state trajectory ($x_1 = C_A - C_{As}$) of the reactor of eq 17 under the LEMPC using the error-triggered online model identification starting from $[C_{As}\ T_s] = [1.2\ \text{kmol/m}^3\ 438.0\ \text{K}]$ with $Q = 4.0 \times 10^4$ kJ/h after the fault.

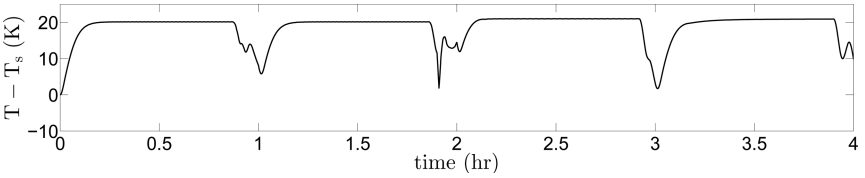

Figure 10. Closed-loop state trajectory ($x_2 = T - T_s$) of the reactor of eq 17 under the LEMPC using the error-triggered online model identification starting from $[C_{As}\ T_s] = [1.2\ \text{kmol/m}^3\ 438.0\ \text{K}]$ with $Q = 4.0 \times 10^4$ kJ/h after the fault.

The initial empirical model utilized within the LEMPC coupled with the moving horizon error detector/online model reidentification strategy was A_1 and B_1. After two operating periods (i.e., at the beginning of the 3rd operating period), an actuator fault occurs, causing the heat input to stay at the value of $Q = 4.0 \times 10^4$ kJ/h for the next two operating periods. As mentioned above, this example assumes that the value at which Q became stuck is unknown, and therefore, the LEMPC continues to solve for both u_1 and u_2 after the fault, but only u_1 is implemented since a fault has occurred in u_2. Figure 6 shows the increase in e_d after the fault occurrence, leading it to eventually exceed its threshold and trigger online model reidentification, using input/output data collected after the occurrence of the fault, which resulted in a sharp drop in the prediction error. The following model was identified using the postfault input/output data:

$$A_2 = \begin{bmatrix} 678.6 \times 10^{-3} & 12.89 \\ -4.378 \times 10^{-3} & 1.168 \end{bmatrix}, B_2 = \begin{bmatrix} 26.35 \times 10^{-3} \\ -1.700 \times 10^{-7} \end{bmatrix} \quad (26)$$

Notably, in accordance with Step 4 of the implementation strategy presented in this work, the B_2 matrix has one less column than the B_1 matrix due to the loss of availability of u_2 as a manipulated input. When the empirical models were reidentified, the controller of eq 21 was replaced with that of eq 24 based on the new empirical model. The same value of $\hat{V}$ was used for all simulations. The input and state trajectories for the reactor process under the LEMPC of eq 6 with the empirical models of eqs 20 and 26 (with the changes in the LEMPC when infeasibility occurs as noted above) subject to the actuator fault in u_2 are presented in Figures 7−10 (u_1 and u_2 in Figures 7 and 8 correspond to the inputs computed by the LEMPC, rather than by the Lyapunov-based control design h_{L1}, and thus the input trajectories have the form shown in the figure because those were the trajectories that the LEMPC determined would maximize the objective function subject to the constraints). Figure 6 shows the value of e_d throughout time under the proposed approach, which shows the growth of e_d that triggered the model reidentification. The new model (A_2 and B_2) that was obtained from input and output data collected after the fault occurrence was able to capture the process dynamics corresponding to the new conditions and caused the values of $e_d(t_k)$ to decrease rapidly afterward. In addition, Figure 11 shows the evolution of the state-space trajectories within the level sets $\Omega_{\hat{\rho}_1}$ and $\Omega_{\hat{\rho}_{e1}}$ during process operation. This figure shows that the state was maintained within

DOI: 10.1021/acs.iecr.7b00576
Ind. Eng. Chem. Res. 2017, 56, 5652−5667

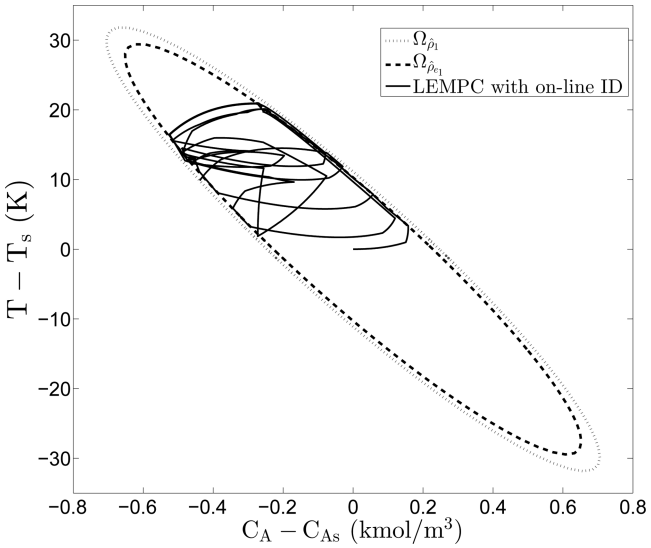

Figure 11. State trajectories in state-space coordinates of the closed-loop CSTR of eq 17 under the LEMPC with error-triggered online model identification starting from $[C_{As}\ T_s]$ = [1.2 kmol/m^3 438.0 K] with $Q = 4.0 \times 10^4$ kJ/h after the fault.

the stability region $\Omega_{\hat{\rho}_1}$ under the proposed scheme. Infeasibility of the LEMPC with the material constraint occurred in the third and fourth hours of operation, during which the material constraint of eq 19 was violated by 0.08 kmol/m^3 and 0.047 kmol/m^3, respectively (i.e., $\frac{1}{1\text{ h}}\int_{2\text{h}}^{3\text{h}} u_1(\tau)\,d\tau = 0.08$ kmol/m^3 for the third hour and $\frac{1}{1\text{ h}}\int_{3\text{h}}^{4\text{h}} u_1(\tau)\,d\tau = 0.047$ kmol/m^3 for the fourth hour), resulting in use of the modified LEMPC design discussed above.

In addition to decreasing the plant−model mismatch due to faults, the online model identification procedure improved the process economic performance compared to not updating the model as presented in Table 4. The results listed are for two approaches: the "One Empirical Model" approach, in which no model reidentification is conducted and the initial empirical model (A_1 and B_1) is used throughout the operating periods, despite the fault (i.e., the LEMPC calculates both u_1 and u_2 despite the fault), and the "Online Model ID" approach, in which the proposed online model reidentification approach is employed. These results show the significant improvement in the profit resulting from updating the empirical model online compared to using the same initial empirical model throughout process operation despite the fault. Table 4 shows the time-averaged profit (denoted by J_e), the maximum value of e_d, and the amount of material used ($\frac{1}{1\text{ h}}\int_{3\text{h}}^{4\text{h}} u_1(\tau)\,d\tau$) for each approach throughout the last hour of operation, where J_e in this table is given by

$$J_e = \frac{1}{1\text{ h}}\int_{3\text{h}}^{4\text{h}} k_0\, e^{-E/R_g T(\tau)}\, C_A{}^2(\tau)\,d\tau \tag{27}$$

Table 4. Relative Prediction Error, Average Profit, and Amount of Material Used for the CSTR under LEMPC during the 4th Hour of Operation

approach	J_e	max $e_d(t_k)$	$\frac{1}{1\text{ h}}\int_{3\text{h}}^{4\text{h}} u_1(\tau)\,d\tau$
One Empirical Model	14.94	3.92	0.089
Online Model ID	15.49	3.01	0.047

To demonstrate the ability of the moving horizon error detector to indicate significant prediction errors and determine when it is necessary to update the model online, another simulation of the CSTR of eq 17 is considered. The CSTR was initialized from the same open-loop stable steady-state and was controlled using the same LEMPC architecture mentioned above with the same initial model (A_1 and B_1). The moving horizon error detector was initiated after $M = 50$ input/output data points were available to calculate the values of e_d. After two operating periods, an actuator fault is assumed to occur causing the heat input to remain at $Q = 1.0 \times 10^4$ kJ/h for the next two operating periods. The LEMPC continued to compute optimal control actions for both u_1 and u_2. This caused values of e_d to increase as can be seen in Figure 12. However, no reidentification was required since the error did not exceed the threshold of $e_d = 3$, showing that the error-triggering was successful at deciding the necessity of model updates. The state-space trajectories of the reactor process under the LEMPC subject to the actuator fault in the value of u_2 are presented in Figure 13. The figure shows that the state was maintained within the stability region even after the fault occurrence. In this simulation, the material constraint was not violated after the fault occurrence (i.e., $\frac{1}{1\text{ h}}\int_{2\text{h}}^{3\text{h}} u_1(\tau)\,d\tau = 0.0$ kmol/m^3 for the third hour and $\frac{1}{1\text{ h}}\int_{3\text{h}}^{4\text{h}} u_1(\tau)\,d\tau = 0.0$ kmol/m^3 for the fourth hour).

To investigate the impact of sensor noise on the error-triggered online model identification procedure for actuator fault compensation, another simulation was performed in which the LEMPC with an empirical model was initialized using A_1 and B_1, and sensor noise was also added to the simulation. The sensor

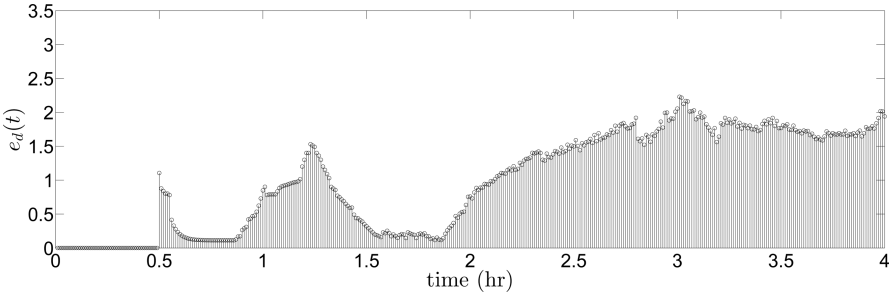

Figure 12. Value of error metric e_d at each sampling time using the detector of eq 25 for the LEMPC integrated with the error-triggered online model identification with $Q = 1.0 \times 10^4$ kJ/h after the fault.

DOI: 10.1021/acs.iecr.7b00576
Ind. Eng. Chem. Res. 2017, 56, 5652−5667

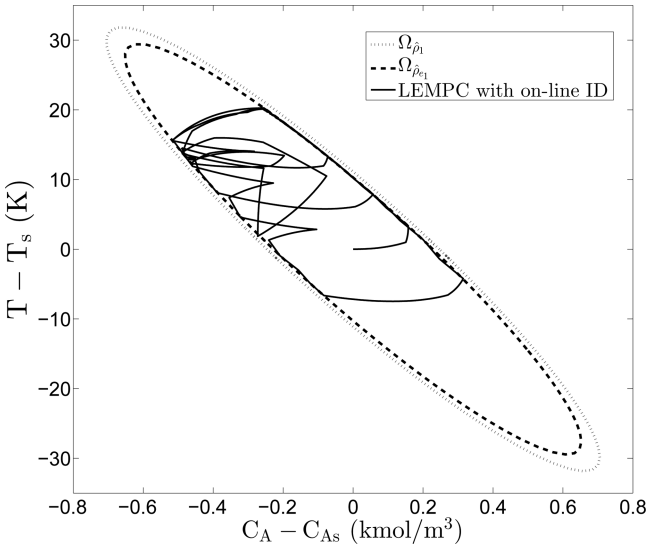

Figure 13. State trajectories in state-space coordinates of the closed-loop CSTR of eq 17 under the LEMPC with error-triggered online model identification starting from $[C_{As}\ T_s] = [1.2\ \text{kmol/m}^3\ 438.0\ \text{K}]$ with $Q = 1.0 \times 10^4$ kJ/h after the fault.

noise was stationary zero-mean Gaussian white noise with a variance of 1 K for the temperature sensor noise and a variance of 0.0625 kmol/m^3 for the concentration sensor noise with bounds on the magnitude of the noise equal to $|w_1(t)| \leq 1$ K and $|w_2(t)| \leq 0.0625$ kmol/m^3. As in the simulations above, a fault in the value of u_2 occurred after two operating periods, causing the value of e_d to increase (as shown in Figure 14) until the error threshold was exceeded, resulting in identification of the following empirical model:

$$A_2 = \begin{bmatrix} 722.1 \times 10^{-3} & 11.17 \\ -3.798 \times 10^{-3} & 1.146 \end{bmatrix}, B_2 = \begin{bmatrix} 24.76 \times 10^{-3} \\ -0.796 \times 10^{-7} \end{bmatrix} \quad (28)$$

Though no filter was applied to obtain this model from the noisy measurements, the model of eq 28 was able to improve the value of J_e, reduce the maximum value of e_d, and reduce the violation of the material constraint in the fourth hour of operation compared to using one empirical model (in the presence of sensor noise) throughout the entire length of operation with the fault (as demonstrated in Table 5).

Infeasibility of the LEMPC with the material constraint in the presence of noise occurred in the third and fourth hours of operation, during which the material constraint of eq 19 was violated by 0.083 kmol/m^3 and 0.051 kmol/m^3, respectively (i.e., $\frac{1}{1\,\text{h}}\int_{2\text{h}}^{3\text{h}} u_1(\tau)\,d\tau = 0.083$ kmol/m^3 for the third hour and $\frac{1}{1\,\text{h}}\int_{3\text{h}}^{4\text{h}} u_1(\tau)\,d\tau = 0.051$ kmol/m^3 for the fourth hour), resulting in use of the modified LEMPC design discussed above. The measured state and input trajectories for the simulation with sensor noise are shown in Figures 15−19.

Table 5. Relative Prediction Error, Average Profit, and Amount of Material Used for the CSTR under LEMPC during the 4th Hour of Operation (Including Sensor Noise)

approach	J_e	max $e_d(t_k)$	$\frac{1}{1\,\text{h}}\int_{3\text{h}}^{4\text{h}} u_1(\tau)\,d\tau$
One Empirical Model	14.92	4.02	0.087
Online Model ID	15.21	3.07	0.051

Remark 12. In the process examples considered in the sections Application of Error-Triggered Online Model Identification When the Fault Value Is Known: Catalytic Process Example and Application of Error-Triggered Online Model Identification When the Fault Value Is Unknown: CSTR Example, the LEMPC's with the empirical models compute time-varying input trajectories and not steady-state input trajectories to optimize the process economics according to the LEMPC optimization problems. The examples indicate that the models constructed from closed-loop data are good in the sense that when these models are used in the EMPC systems, the moving horizon error detector triggers model reidentification infrequently and the process economics improve when the models are updated compared to not updating the empirical models, which means that the LEMPC inputs sufficiently excite the closed-loop process to produce process data suitable for model construction.

CONCLUSION

In this work, we proposed an online model identification methodology that updates the empirical models used in LEMPC online to overcome actuator faults. Empirical models were updated online based on significant prediction errors indicated by a moving horizon error detector. The error-triggered online model identification methodology can be applied to overcome different actuator fault scenaria that occur in practice, including the case where the value at which the actuator is stuck is known and the case where the value at which the actuator is stuck is unknown. Applications were demonstrated for both cases using two chemical process examples under LEMPC. In the first example, a benchmark chemical process was used to demonstrate the application of the proposed scheme in the case where the value at which the actuator is stuck is known. In the second example, another chemical process was used to demonstrate the

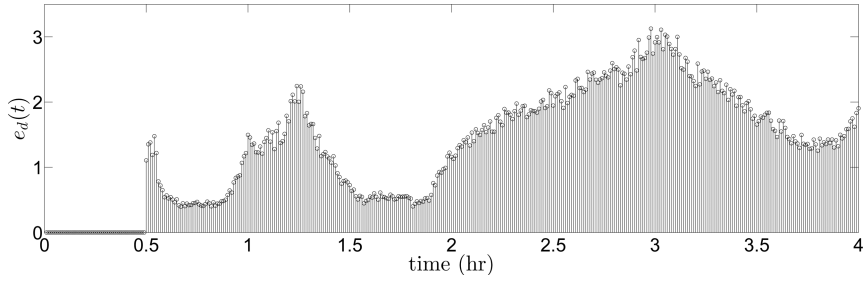

Figure 14. Value of error metric e_d at each sampling time using the detector of eq 25 for the LEMPC integrated with the error-triggered online model identification with $Q = 4.0 \times 10^4$ kJ/h after the fault (including sensor noise).

DOI: 10.1021/acs.iecr.7b00576
Ind. Eng. Chem. Res. 2017, 56, 5652−5667

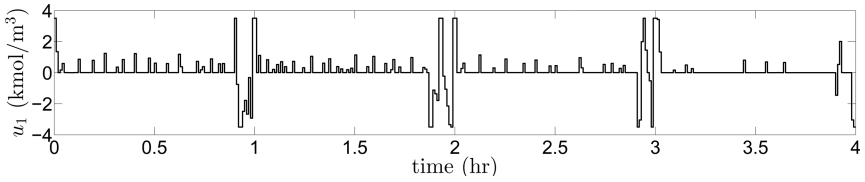

Figure 15. Closed-loop input trajectory ($u_1 = C_{A0} - C_{A0s}$) of the reactor of eq 17 under the LEMPC using the error-triggered online model identification starting from $[C_{As}\ T_s] = [1.2\ \text{kmol/m}^3\ 438.0\ \text{K}]$ with $Q = 4.0 \times 10^4$ kJ/h after the fault (including sensor noise).

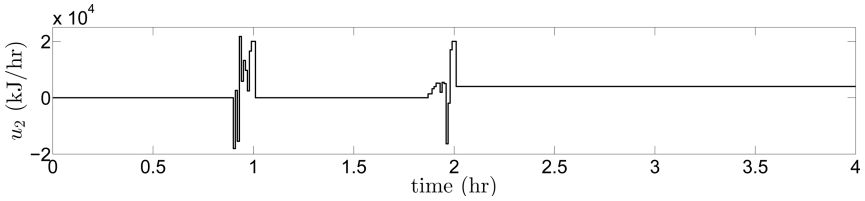

Figure 16. Closed-loop input trajectory ($u_2 = Q - Q_s$) of the reactor of eq 17 under the LEMPC using the error-triggered online model identification starting from $[C_{As}\ T_s] = [1.2\ \text{kmol/m}^3\ 438.0\ \text{K}]$ with $Q = 4.0 \times 10^4$ kJ/h after the fault (including sensor noise).

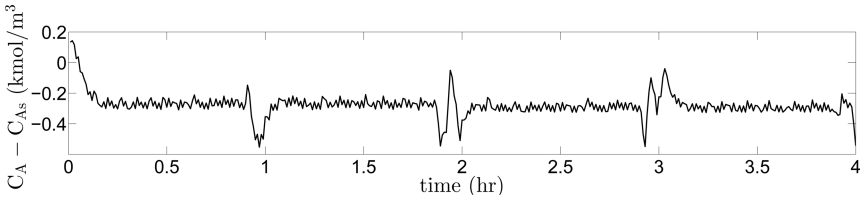

Figure 17. Closed-loop state trajectory ($x_1 = C_A - C_{As}$) of the reactor of eq 17 under the LEMPC using the error-triggered online model identification starting from $[C_{As}\ T_s] = [1.2\ \text{kmol/m}^3\ 438.0\ \text{K}]$ with $Q = 4.0 \times 10^4$ kJ/h after the fault (including sensor noise).

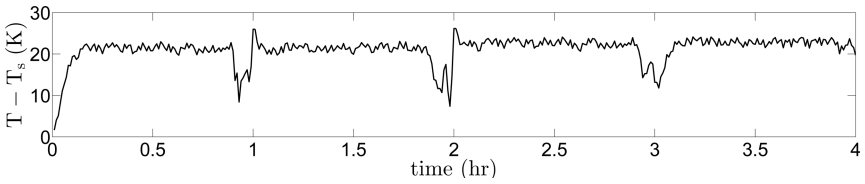

Figure 18. Closed-loop state trajectory ($x_2 = T - T_s$) of the reactor of eq 17 under the LEMPC using the error-triggered online model identification starting from $[C_{As}\ T_s] = [1.2\ \text{kmol/m}^3\ 438.0\ \text{K}]$ with $Q = 4.0 \times 10^4$ kJ/h after the fault (including sensor noise).

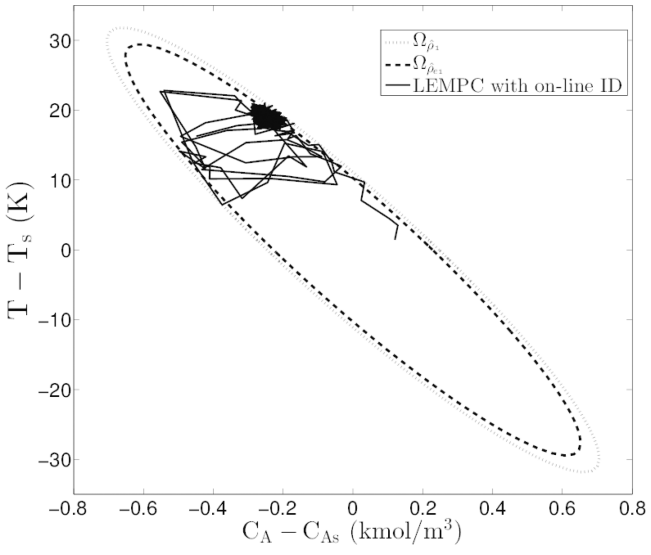

Figure 19. State trajectories in state-space coordinates of the closed-loop CSTR of eq 17 under the LEMPC with error-triggered online model identification starting from $[C_{As}\ T_s] = [1.2\ \text{kmol/m}^3\ 438.0\ \text{K}]$ with $Q = 4.0 \times 10^4$ kJ/h after the fault (including sensor noise).

application of the proposed scheme in the case where the value at which the actuator is stuck is unknown. The chemical process examples presented the ability of the proposed scheme to detect when it is necessary to update the empirical model online in response to operational variations caused by actuator faults and/or disturbances. Improved state predictions and economic performance were obtained under the proposed scheme compared to using one empirical model throughout operation despite the actuator faults. The examples show the successful implementation of a unified framework using the moving horizon error detector and error-triggered model updates within LEMPC for handling faults. Future research on this topic may investigate the use of nonlinear or stochastic empirical models in the error-triggered online model identification strategy instead of deterministic linear empirical models. It may also further examine the need to wait to change the model or error detector parameters immediately after the fault until sufficient data is available, and the requirement that the inputs be time-varying to excite the dominant process dynamics when all actuators are online and also as various actuators are taken off-line due to faults to allow routine process operating data to be available to be utilized to identify sufficiently accurate empirical models.

DOI: 10.1021/acs.iecr.7b00576
Ind. Eng. Chem. Res. 2017, 56, 5652−5667

AUTHOR INFORMATION

Corresponding Author

*E-mail: pdc@seas.ucla.edu.

ORCID

Panagiotis D. Christofides: 0000-0002-8772-4348

Notes

The authors declare no competing financial interest.

ACKNOWLEDGMENTS

Financial support from the National Science Foundation and the Department of Energy is gratefully acknowledged.

REFERENCES

(1) Ellis, M.; Durand, H.; Christofides, P. D. A tutorial review of economic model predictive control methods. *J. Process Control* **2014**, *24*, 1156−1178.

(2) Amrit, R.; Rawlings, J. B.; Angeli, D. Economic optimization using model predictive control with a terminal cost. *Annual Reviews in Control* **2011**, *35*, 178−186.

(3) Heidarinejad, M.; Liu, J.; Christofides, P. D. Economic model predictive control of nonlinear process systems using Lyapunov techniques. *AIChE J.* **2012**, *58*, 855−870.

(4) Huang, R.; Harinath, E.; Biegler, L. T. Lyapunov stability of economically oriented NMPC for cyclic processes. *J. Process Control* **2011**, *21*, 501−509.

(5) Ogunnaike, B. A.; Ray, W. H. *Process Dynamics, Modeling, and Control*; Oxford University Press: New York, NY, 1994.

(6) Anderson, S. R.; Kadirkamanathan, V. Modelling and identification of non-linear deterministic systems in the delta-domain. *Automatica* **2007**, *43*, 1859−1868.

(7) Van Overschee, P.; De Moor, B. *Subspace Identification for Linear Systems: Theory, Implementation, Application*; Kluwer Academic Publishers: Boston, MA, 1996.

(8) Verhaegen, M.; Dewilde, P. Subspace model identification Part 1. The output-error state-space model identification class of algorithms. *Int. J. Control* **1992**, *56*, 1187−1210.

(9) Favoreel, W.; De Moor, B.; Van Overschee, P. Subspace state space system identification for industrial processes. *J. Process Control* **2000**, *10*, 149−155.

(10) Viberg, M. Subspace-based methods for the identification of linear time-invariant systems. *Automatica* **1995**, *31*, 1835−1851.

(11) Huang, B.; Kadali, R. *Dynamic Modeling, Predictive Control and Performance Monitoring: A Data-driven Subspace Approach*; Springer-Verlag: London, 2008.

(12) Van Overschee, P.; De Moor, B. N4SID: Subspace algorithms for the identification of combined deterministic-stochastic systems. *Automatica* **1994**, *30*, 75−93.

(13) Larimore, W. E. Canonical Variate Analysis in identification, filtering, and adaptive control. In *Proceedings of the 29th Conference on Decision and Control*; Honolulu, HI, 1990, pp 596−604.

(14) Markovsky, I.; Willems, J. C.; Rapisarda, P.; De Moor, B. L. M. Algorithms for deterministic balanced subspace identification. *Automatica* **2005**, *41*, 755−766.

(15) Alanqar, A.; Ellis, M.; Christofides, P. D. Economic model predictive control of nonlinear process systems using empirical models. *AIChE J.* **2015**, *61*, 816−830.

(16) Lao, L.; Ellis, M.; Christofides, P. D. Proactive fault-tolerant model predictive control. *AIChE J.* **2013**, *59*, 2810−2820.

(17) Mhaskar, P.; Gani, A.; El-Farra, N. H.; McFall, C.; Christofides, P. D.; Davis, J. F. Integrated fault-detection and fault-tolerant control of process systems. *AIChE J.* **2006**, *52*, 2129−2148.

(18) Massera, J. L. Contributions to stability theory. *Annals of Mathematics* **1956**, *64*, 182−206.

(19) Khalil, H. K. *Nonlinear Systems*, 3rd ed.; Prentice Hall: Upper Saddle River, NJ, 2002.

(20) Lin, Y.; Sontag, E. D. A universal formula for stabilization with bounded controls. *Systems & Control Letters* **1991**, *16*, 393−397.

(21) El-Farra, N. H.; Christofides, P. D. Bounded robust control of constrained multivariable nonlinear processes. *Chem. Eng. Sci.* **2003**, *58*, 3025−3047.

(22) Christofides, P. D.; El-Farra, N. H. *Control of Nonlinear and Hybrid Process Systems: Designs for Uncertainty,Constraints and Time-Delays*; Springer-Verlag: Berlin, Germany, 2005.

(23) Muñoz de la Peña, D.; Christofides, P. D. Lyapunov-based model predictive control of nonlinear systems subject to data losses. *IEEE Trans. Autom. Control* **2008**, *53*, 2076−2089.

(24) Alanqar, A.; Durand, H.; Christofides, P. D. Error-triggered on-line model identification for model-based feedback control. *AIChE J.* **2017**, *63*, 949−966.

(25) Özgülşen, F.; Adomaitis, R. A.; Çinar, A. A numerical method for determining optimal parameter values in forced periodic operation. *Chem. Eng. Sci.* **1992**, *47*, 605−613.

(26) Bailey, J. E.; Horn, F. J. M.; Lin, R. C. Cyclic operation of reaction systems: Effects of heat and mass transfer resistance. *AIChE J.* **1971**, *17*, 818−825.

(27) Paduart, J.; Lauwers, L.; Swevers, J.; Smolders, K.; Schoukens, J.; Pintelon, R. Identification of nonlinear systems using Polynomial Nonlinear State Space models. *Automatica* **2010**, *46*, 647−656.

(28) Alanqar, A.; Durand, H.; Christofides, P. D. On identification of well-conditioned nonlinear systems: Application to economic model predictive control of nonlinear processes. *AIChE J.* **2015**, *61*, 3353−3373.

(29) Alfani, F.; Carberry, J. J. An exploratory kinetic study of ethylene oxidation over an unmoderated supported silver catalyst. *Chim. Ind.* **1970**, *52*, 1192−1196.

(30) Wächter, A.; Biegler, L. T. On the implementation of an interior-point filter line-search algorithm for large-scale nonlinear programming. *Mathematical Programming* **2006**, *106*, 25−57.

DOI: 10.1021/acs.iecr.7b00576
Ind. Eng. Chem. Res. 2017, 56, 5652−5667